Pro42 and Val45 of staphylokinase modulate intermolecular interactions of His43–Tyr44 pair and specificity of staphylokinase–plasmin activator complex

ARTICLE *in* FEBS LETTERS · FEBRUARY 2012

Impact Factor: 3.17 · DOI: 10.1016/j.febslet.2012.01.046 · Source: PubMed

3 AUTHORS, INCLUDING:

Ashish Ashish
Institute of Microbial Technology
48 PUBLICATIONS **487** CITATIONS
SEE PROFILE

Kanak Dikshit
Institute of Microbial Technology
54 PUBLICATIONS **1,235** CITATIONS
SEE PROFILE

FEBS Letters 586 (2012) 653–658

journal homepage: www.FEBSLetters.org

Pro^{42} and Val^{45} of staphylokinase modulate intermolecular interactions of His^{43}–Tyr^{44} pair and specificity of staphylokinase–plasmin activator complex

Satish Singh, Ashish, Kanak L. Dikshit *

Institute of Microbial Technology, CSIR, Sector-39 A, Chandigarh 160036, India

ARTICLE INFO

Article history:
Received 15 December 2011
Accepted 19 January 2012
Available online 2 February 2012

Edited by Richard Cogdell

Keywords:
Staphylokinase
Plasminogen activation
Molecular modeling
Site-directed mutagenesis
Enzyme–substrate complex
Protein–protein interaction

ABSTRACT

Staphylokinase (SAK) forms a 1:1 stoichiometric complex with plasmin (Pm) and changes its substrate specificity to create a plasminogen (Pg) activator complex. The His^{43}–Tyr^{44} pair of SAK resides within the active site cleft of the partner Pm and generates intermolecular contacts to confer Pg activator ability to the SAK–Pm bimolecular complex. Site-directed mutagenesis and molecular modeling studies unravelled that mutation at 42nd or 45th positions of SAK specifically disrupts cation-pi interaction of His^{43} with Trp^{215} of partner Pm within the active site, whereas pi–pi interaction of Tyr^{44} with Trp^{215} remain energetically favoured.

Structured summary of protein interactions:
Pg binds to **SAK** by surface plasmon resonance (View Interaction: 1, 2, 3)
SAK enzymaticly reacts **Pg** by enzymatic study (View Interaction: 1, 2, 3, 4, 5)

1. Introduction

Staphylokinase (SAK), a 15.5 kDa fibrinolytic protein secreted from the bacterium, *Staphylococcus aureus* [1,2], is a plasminogen (Pg) activator that induces fibrin specific thrombolysis in human plasma [3,4]. Unlike direct human Pg activators such as tissue-plasminogen activator (t-PA) [5] and urokinase (UK), SAK does not have any proteolytic activity of its own but it acts by forming a 1:1 stoichiometric complex with plasmin (Pm) and changing its substrate specificity to activate Pg as its substrate [6,7]. Unlike SAK, Streptokinase (SK) can form a functional activator complex with Pg by modifying its active site without any proteolytic cleavage in Pg molecule [8] while SAK requires the conversion of SAK–Pg complex to SAK–Pm [9] and the removal of ten amino acid residues from the N-terminus to form a functional Pg activator complex [10,11]. Despite these differences in their mechanism of Pg activation, a close structural homology exists between SAK and α domain of SK [12] and their intermolecular contacts with the partner [13–15] near the active site suggesting that the critical contacts at the two respective interfaces have been well conserved in the evolutionary process and may be crucial in Pg binding and activation [12].

The mechanisms by which SAK reprograms the broad trypsin like substrate specificity of Pm in SAK–Pm complex towards sessile peptide bond of Arg^{561}–Val^{562} within the activation loop of substrate Pg is a fascinating aspect of SAK functionality that has not been understood at the molecular level. The crystal structure of ternary complex of SAK, complexed with the partner and substrate μPm [14], has revealed several intermolecular contacts between SAK and the partner μPm molecule in the vicinity of its active site. More or less similar intermolecular interactions occur when SK forms a bimolecular Pg activator complex with Pg/Pm [15,16]. Recent site-directed mutagenesis and molecular modeling studies, conducted in our laboratory, have demonstrated that His^{43}–Tyr^{44} pair of SAK generates crucial contacts at the interface with the partner Pm molecule and may be vital for the specificity switch and functionality of binary activator complex of SAK with Pm [17]. Structural comparison of unbound SAK with the bound one in the SAK–μPm complex revealed distinct movement of Ser^{41}–His^{43} region after complex formation with Pm indicating the involvement of Pro^{42} at this junction. Moreover, Val^{45} another flanking residue of this pair is present at the crucial junction of intermolecular contacts. Biochemical and molecular modeling studies, presented in this work, demonstrated key role of SAKPro^{42} and SAKVal^{45} in modulating the intermolecular interactions of His^{43} and Tyr^{44} residues of SAK with the partner and specificity of the SAK–Pm complex.

2. Materials and methods

2.1. Bacterial strains, plasmids and reagents

The expression vector pET9b and *Escherichia coli* host strains, JM109 and BL21DE3, purchased from Promega (WI, USA), were

* Corresponding author. Fax: +91 172 2690585.
E-mail address: kanak@imtech.res.in (K.L. Dikshit).

0014-5793/$36.00 © 2012 Federation of European Biochemical Societies. Published by Elsevier B.V. All rights reserved.
doi:10.1016/j.febslet.2012.01.046

routinely utilized for cloning and expression of recombinant genes using *sak* gene [11,18] as a template. All restriction and modifying enzymes were procured from New England Biolabs or Stratagene (USA). Chromozyme PL (Tosyl-glycyl-polyl-lysine-4-nitranilide-acetate) and human Glu-Pg was obtained from Roche Diagnostics (Germany). Human Pg was also purified from human plasma using Lysine-Sepharose chromatography [19].

2.2. Site-directed mutagenesis of SAK: expression and purification SAK mutants

Site directed mutagenesis of Pro^{42} and Val^{45} residues of SAK was done by using pRM1 plasmid as template through QuickChange site directed mutagenesis kit from Stratagene which uses a set of two primers having the desired mutation in the center. List of oligonucleotide primers used for this purpose is given in Supplementary Table S1. Site directed mutants of SAK were cloned, expressed in *E. coli* and purified as described previously [17].

2.3. Pg activation property of SAK/SAK mutants

To check the Pg activation properties of SAK mutants, 5 nM SAK or SAK mutants were mixed with 1.5 μM Pg in assay buffer (50 mM Tris·HCl, pH 7.5, containing 0.1% BSA, 100 mM NaCl and 0.01% Tween 80) containing 1 mM chromozyme in 96 well microtitre plate and generation of Pm was measured as a function of time at 405 nm at 25 °C in BioTEK Powerwave X 96 wells microtitre plate reader [11,20]. To see the Pg activation by preformed complexes of SAK or SAK mutants with Pm, equimolar mixtures of SAK or SAK mutants (0.5 μM) and Pm (0.5 μM) were preincubated in assay buffer at 37 °C for 5 min to generate the SAK–Pm bimolecular complex. These preformed activator complexes (5 nM) were then mixed with substrate Pg (1.5 μM) and generation of Pm was measured spectrophotometrically at 25 °C using Chromozyme PL (1 μM) as described previously [11,18]. To calculate the steady-state kinetic constants, these preformed complex of SAK–Pm (5 nM) were mixed with different concentrations of Pg (0.5–5 μM) and 1.0 mM Chromozyme PL. The change in absorbance at 405 nm was measured as a function of time at 25 °C as described above. The kinetic constants were determined through Michaelis Menten plot [18,21].

2.4. Amidolysis profile of SAK–Pm bimolecular complex

To see the specificity of the active site generated by SAK/SAK mutants with Pm, an equimolar mixture of Pm (0.5 μM) with SAK/SAK mutant (0.5 μM) in the reaction buffer (50 mM Tris·HCl, pH 7.5, containing 0.1% BSA, 100 mM NaCl) was incubated for 5 min and then 50 nM of the SAK/SAK mutant–Pm complex was added to the reaction buffer containing 1.5 μM Chromozyme in microtitre plate. The amidolysis profile of SAK or SAK mutants was measured spectrophotometrically at 405 nm in microtitre plate as described above [22].

2.5. Determination of the binding affinity of SAK/SAK mutants for Pg by surface plasmon resonance (SPR)

The kinetic constants for binding of SAK/SAK mutants with Pg were determined by SPR [23] using Sensor Chip SA in a BIACORE 3000 biosensor [24]. Pg was purified from human plasma and biotinylated with Sulpho-NHS-LC-Biotin [25]. Approximately 1500 Resonance units of Pg were immobilized on Sensor Chip SA. To calculate the rate and equilibrium binding constants, the different concentrations of SAK/SAK mutants (1–20 μM or 10–100 μM) were passed over the immobilized Pg. All the experiments were performed in HBS running buffer (20 mM HEPES, 1 mM EDTA, 0.15 M NaCl, and 0.005% surfactant P20, pH 7.2) supplemented with NPGB to avoid any Pg/Pm mediated proteolysis [22]. The k_{on} (assosciation rate constant, k_a), k_{off} (dissociation rate constant, k_d) and K_D (equilibrium binding constant) values were calculated by non-linear fitting of the association and dissociation curves using 1:1 Langmuir binding model in BIACORE 3000 evaluation software.

2.6. Molecular modeling studies of SAK/SAK mutants –μPm complex

Energy minimization of the coordinates of SAK (and its mutants) in complex with μPm was carried out using Newton software in the Tinker suite of programs [26,27]. Using the crystal structure 1BUI as starting coordinates, the substrate μPm was excluded from calculations to mimic the binary activator complex. Mutants were generated using SPDB viewer program and all rotameric conformations of each mutant for the side-chain with least disallowed contacts [28] were selected. The calculations were carried out employing implicit dielectric of 80, vdw-cutoff of 9 Å and force-field parameters of optimized parameters for liquid simulation united-atom (OPLSUA). Coordinates were minimized to an RMSD cut-off of 0.01 kcal/mol/Å. Total and interaction energies were estimated using Analyze program.

3. Results

3.1. Intermolecular contacts at the interface of active site of SAK–μPm bimolecular complex

$His^{43}$and Tyr^{44} residues of SAK are uniquely placed inside the active site of μPm in SAK–Pm complex and interact with Trp^{215} (Fig. 1A) through cation–pi and pi–pi interactions respectively. Presence of His^{43}–Tyr^{44} pair in SAK and Lys^{36}–Phe^{37} in SK and their contacts at the two respective interfaces (Fig. 1B) signifies similarity between these interactions that may be required for changing the specificity of active site towards Pg activation. Positioning of Pro^{42} and Val^{45} of SAK at the junction of these crucial interactions led to the speculation that these two residues may be involved in the spatial arrangement of their neighbors for establishing their intermolecular contacts with the partner Pm.

3.2. Site-directed mutagenesis of $SAKPro^{42}$ and $SAKVal^{45}$ and functional properties of SAK mutants

To gain experimental insights for the role of Val^{45} and Pro^{42} in Pg binding and activation, the specific mutants of these residues were generated. Val^{45} residue of SAK was replaced either with Ala in $SAKVal^{45}Ala$ mutant, or Tyr in $Val^{45}Tyr$ mutant. Pro^{42} was mutated to leucine in $SAKPro^{42}Leu$ mutant and a double mutant namely $Tyr^{44}Phe$, $Val^{45}Phe$ was constructed in which both SAK-Tyr^{44} and $SAKVal^{45}$ were mutated to phenylalanine respectively to mimic the residues as present in SK. Surprisingly, all the mutants showed much diminished Pg activation ability as compared to native SAK as evident from their activation profile (Fig. 2A). When preformed complexes of $SAKPro^{42}$ and Val^{45} were used with Pm, these complexes exhibited extremely slow progression and a significant lag (10 min as compared to 2 min in native SAK) in Pg activation suggesting attenuation in catalytic activity of activator complexes formed by these SAK mutants (Fig. 2B).

3.3. Steady state kinetics of Pg activation by equimolar complexes of SAK or $SAKPro^{42}$/$SAKVal^{45}$ mutants with Pm

The k_m and k_{cat} values of Pg activation by $SAKPro^{42}$ and SAK-Val^{45} mutants (Table 1) clearly suggested the crucial role of these residues in complex formation and activation of Pg. These observa-

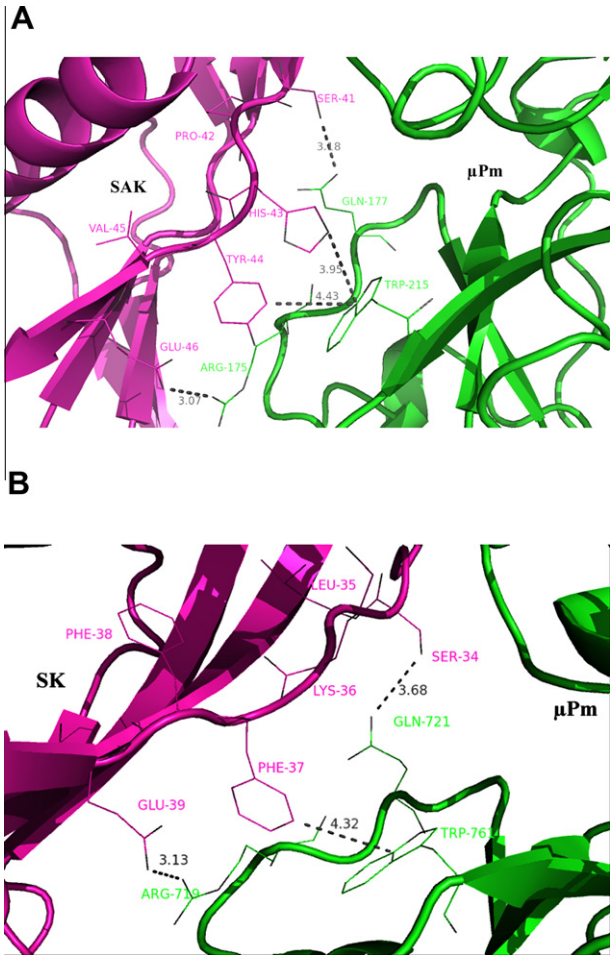

Fig. 1. Structural features of interface of the (A) SAK–μPm (B) SK–μPm bimolecular complex. Ribbon diagram representation of SAK–μPm and SK–μPm complex displays interacting amino acids as lines and interatomic distances as dotted lines. The figure was prepared by PyMol software (http://www.pymol.org).

tions clearly indicated that Pro^{42}/Val^{45} residue at this position may be required for the optimal Pg activation by SAK–μPm bimolecular complex and could not be replaced by any other residue for generating a functional binary activator complex.

3.4. Amidolytic activity of precomplexes of SAK/SAK mutants with Pm

$SAKVal^{45}$ and $SAKPro^{42}$ mutants were less efficient in generating the active site specificity of Pm as compared to native SAK as evident from their amidolytic activity (Fig. 3). These results clearly demonstrated that the loss of the Pg activation ability of these mutants was due to loss of proper active site exposure in the precomplexes of these mutants with Pm.

3.5. Binding affinity measurement of SAK/$SAKPro^{42}$/$SAKVal^{45}$mutants with Pg using SPR

To explore the relative binding affinities of these mutants for Pg/Pm in order to explain further the underlying cause of decreased catalytic potential of SAK mutants, real-time SPR studies were done. The binding of Pm on the surface of biacore chip was not satisfactorily obtained after several attempts, thus, affinity of SAK mutants with only full length Pg molecule was determined. The association/dissociation rate constants (k_{on}/k_{off}) and equilibrium binding constant (K_D) of SAK and Val^{45}Tyr with Pg are summarized in Table 2. However, the binding constants could not be calculated for Val^{45}Ala and Pro^{42}Leu mutants as the sensorgrams of these mutants showed almost no binding. The representative sensorgram for SAK/SAK mutant–Pg interaction are shown in supplementary data (Supplementary Fig. S1, S2). The K_D values of SAK mutants showed a significant decrease in their binding affinity for Pg to form bimolecular complex as compared to SAK.

Thus, the overall experimental data suggested the crucial role of $SAKPro^{42}$ and Val^{45} in Pg binding and activation.

3.6. Energy minimization and molecular modeling studies

Four in silico mutants of $SAKPro^{42}$ and $SAKVal^{45}$ i.e. single mutants namely Pro^{42}Leu, Val^{45}Ala and Val^{45}Tyr and a double mutant Tyr^{44}Phe/Val^{45}Phe were generated using the ternary complex of SAK and μPm (PDB ID: 1BUI) as the starting structure to explore the role of these residues in forming a functional bimolecular complex. Interestingly, energy minimization studies of the binary complex of SAK mutant–μPm showed that any alteration at these two topological positions of SAK i.e. 42nd and 45th led to alterations in the local environment of His^{43}–Tyr^{44} pair. The energy minimized coordinates for all the mutants were aligned at Cα chain of Pro^{42} to Tyr^{44} of SAK to show the relative movement of the participating residues (Fig. 4). Recently, based on experimental and

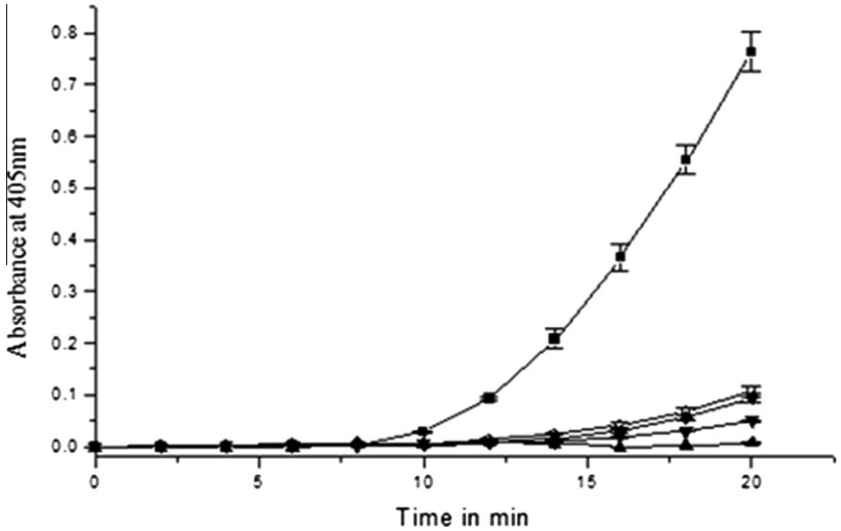

Fig. 2a. Pg activation profile of SAK/SAK mutants. The graph shows SAK (-■-), $SAKPro^{42}$Leu (-○-), $SAKVal^{45}$Ala (-♦-), $SAKVal^{45}$Tyr (-▼-), and $SAKTyr^{44}$Phe,Val^{45}Phe, (-▲-).

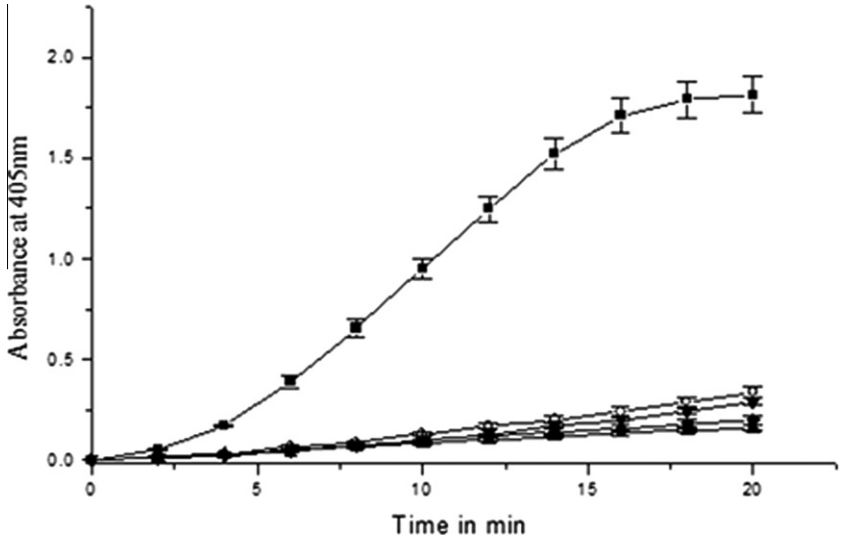

Fig. 2b. Pg activation profile by pre-formed bimolecular complexes of SAK and its mutants. The graph shows SAK (-■-), SAKPro^{42}Leu (-○-), SAKVal^{45}Ala (-♦-), SAKVal^{45}Tyr (-▼-), and SAKTyr^{44}Phe,Val^{45}Phe, (-▲-).

Table 1
Steady-state kinetic constants for the Pg activation properties of equimolar complexes of SAKPro^{42} and SAKVal^{45} mutants and Pm.

Bimolecular complex	k_m[a] (μM)	k_{cat}[a] (s^{-1})	k_{cat}/k_m (s^{-1} μM^{-1})
SAK–Pm	0.70 ± 0.09	0.43 ± 0.06	0.61
SAKPro^{42}Leu–Pm	2.0 ± 0.1	0.05 ± 0.007	0.025
SAKVal^{45}Ala–Pm	1.9 ± 0.08	0.066 ± 0.006	0.034
SAKVal^{45}Tyr–Pm	2.2 ± 0.1	0.1 ± 0.03	0.045
SAKTyr^{44}Phe,Val^{45}Phe,–Pm	4.2 ± 0.1	0.01 ± 0.002	0.002

[a] The results are means ± S.E.M. of three determinations.

Table 2
The binding affinity constants of Pg for SAK and its mutants measured through SPR by 1:1 Langmuir binding model.

Bimolecular complex	k_a[a] ($\times 10^2$) (M^{-1} s^{-1})	k_d[a] ($\times 10^{-3}$)(s^{-1})	K_D[a] ($\times 10^{-6}$) (M)
SAK–Pg	3.1 ± 0.2	3.3 ± 0.3	11 ± 0.5
SAKVal^{45}Tyr–Pg	0.9 ± 0.3	5.4 ± 0.4	60 ± 0.8
SAKPro^{42}Leu–Pg[b]	–[b]	–[b]	–[b]
SAKVal^{45}Ala–Pg[b]	–[b]	–[b]	–[b]

[a] The results are means ± S.E.M. of three determinations.
[b] The binding constants could not be determined due to very poor binding as shown in the sensorgram (Supplemntary Fig. S2).

theoretical results, we reported that these two residues i.e. His^{43} and Tyr^{44} are the key regulators of the specificity switch [17]. In the energy minimized coordinates of SAKPro^{42}Leu mutant, the crucial native-like cation–pi interaction of SAKHis^{43}–μPmTrp^{215} pair at the interface was completely lost as the side-chains significantly moved away as shown by the distance measurements (Table 3). Similarly, coordinates of Val^{45}Tyr mutation showed the displacement of His^{43} of SAK away from Trp^{215} of μPm by more than 1 Å. In sharp contrast, Val^{45}Ala mutant lacked any significant changes in the local environment. Interestingly, all these mutations did not affect much the relative position and orientation of Tyr^{44} and Glu^{46} to disrupt any major interaction of these residues with μPm.

Energy minimization studies were further extended to visualize the structural changes in double mutants of SAK i.e. His^{43}KVal^{45}Tyr and His^{43}LysVal^{45}Ala. In energy minimized coordinates of His^{43}KVal^{45}Tyr mutant, Lys^{43} was not able to interact with either Glu^{180}

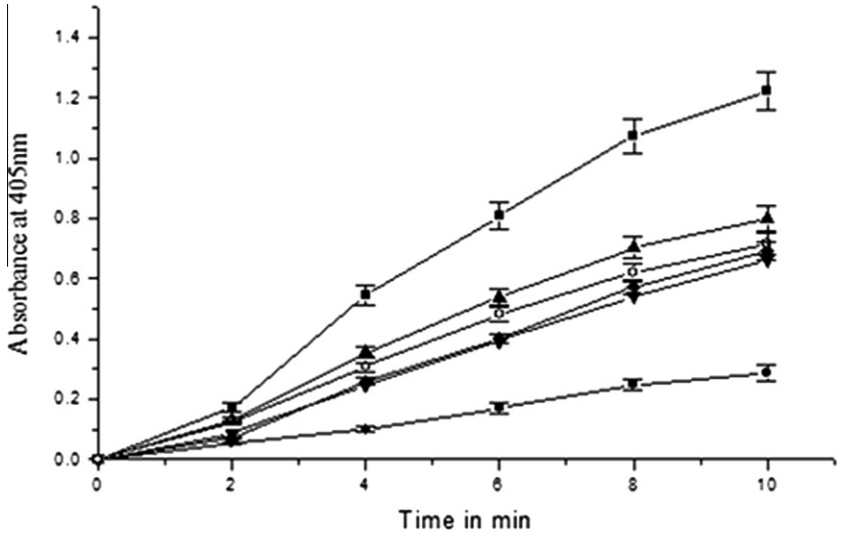

Fig. 3. Amidolysis profile of equimolar mixture of SAK/SAK mutants with Pm using Chromozyme PL. The graph shows Pm alone (-■-), SAK (-●), SAKPro^{42}Leu(-▲-), SAKVal^{45}Ala (-▼-) and SAKVal^{45}Tyr (-♦-), SAKTyr^{44}Phe,Val^{45}Phe.

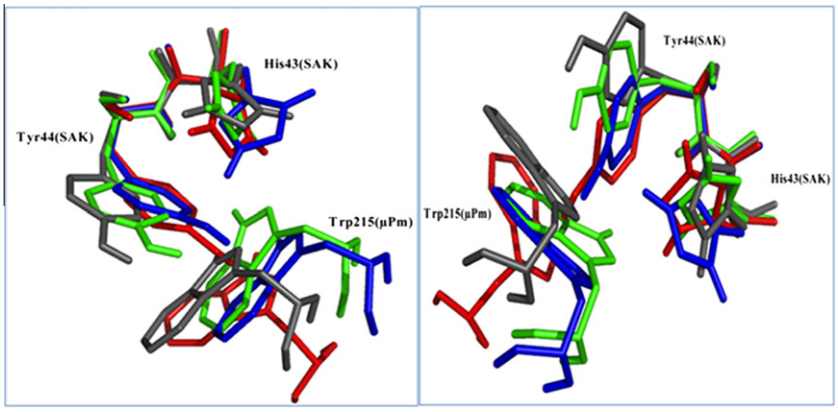

Fig. 4. Molecular modeling of interaction of SAK/SAK mutants at the interface after energy minimization of SAK–μPm binary complex. This figure shows how in silico mutation at Pro^{42} and Val^{45} of SAK positions $SAKHis^{43}$ in a non-interacting fashion away from $\mu PmTrp^{215}$. The interacting residues are represented as sticks in SAK as green, $Pro^{42}Leu$ as red, $Val^{45}Ala$ as blue and $Val^{45}Tyr$ as gray.

Table 3
Interatomic distances between His^{43} of SAK and Trp^{215} of μPm in SAK-μPm binary complex after energy minimization.

Participating atoms of $SAKHis^{43}$–$\mu PmTrp^{215}$ pair	SAK/SAK mutant (distance in Å)			
	SAK	$Pro^{42}Leu$	$Val^{45}Ala$	$Val^{45}Tyr$
CE1–NE1	4.5	6.17	4.37	5.49
ND1–CD1	3.33	5.71	4.28	4.85
CE1–CD1	3.68	5.86	3.41	4.51

or Trp^{215} of μPm as found in our previous studies. Surprisingly, in $His^{43}LysVal^{45}Ala$ mutant, Tyr^{44} of SAK moved away from Trp^{215} of μPm to disrupt pi–pi interactions between the two aromatic rings.

Thus, Molecular modeling studies suggested the role of Pro^{42} and Val^{45} in stabilizing the crucial interactions of His^{43}–Tyr^{44} pair of SAK with Trp^{215} of μPm.

4. Discussion

High affinity intermolecular interactions between SAK and Pm in SAK–Pm binary activator complex change the broad substrate specificity of the Pm active site towards specific recognition of activation loop of Pg for its catalysis. The dramatic macromolecular substrate specificity change that Pm exhibits after SAK binding depends primarily on its precise interactions with its partner. His^{43} and Tyr^{44} residues of SAK occupy a unique position near the active site of partner Pm [14] and generate contacts with the partner that has been shown to modulate specificity and Pg activator activity of SAK–Pm bimolecular complex. The present experimental and modeling studies have demonstrated that precise positioning and interactions of His^{43}–Tyr^{44} pair of SAK at the interface of SAK–Pm enzyme complex are modulated by its flanking residues, Pro^{42} and Val^{45} that may be vital for the SAK mediated Pg activation.

Although crystal structure of SAK–μPm ternary complex does not display any direct contacts of Pro^{42} and Val^{45} residues of SAK with the partner μPm, any mutation at these positions resulted in drastic reduction in Pg activator ability of SAK–Pm complex. Steady-state kinetics and SPR studies suggested that these SAK mutants are unable to generate proper intermolecular interactions with the partner Pm that subsequently can impair substrate Pg catalysis. These results validated that the impairment in the Pg activation ability of these mutants is primarily due to the lesion in their ability to interact correctly with the partner to generate a binary complex having optimal specificity towards Pg. Molecular modeling studies substantiated that mutation at these two critical positions i.e. Pro^{42} and Val^{45} may disrupt cation–pi interactions between His^{43} of SAK and Trp^{215} of partner Pm. The experimental data indicated significant reduction in the Pg activator ability of this $SAKVal^{45}Ala$ mutant but it is likely that the present modeling approach is unable to trap the structural perturbations within this region due to $Val^{45}Ala$ mutation. Interestingly, none of these SAK mutants displayed any major effect on intermolecular contact of Tyr^{44} with Trp^{215} of Pm at the interface suggesting that the flanking residues of His^{43}–Tyr^{44} pair are crucial for the correct positioning and fine adjustment of His^{43} within the active site of SAK–Pm complex for the specificity of Pm active site.

The pi–pi stacking and cation–pi interactions are important components of stabilizing force and structural architecture of many protein–protein complexes [29] as in SAK–Pm and SK–Pm complex. Disruption of any one of these two contacts in the SAK–Pm complex abrogated its Pg activator activity suggesting the requirement of His^{43} and Tyr^{44} for the function of SAK. Our previous observations as well as the present study revealed that the position of His^{43} is more vulnerable to local changes at the active site as compared to Tyr^{44} due to lower strength of interaction with aromatic ring as compared to other positively charged residues.

The present experimental and molecular modeling studies have unravelled that Pro^{42} and Val^{45} of SAK play a crucial role in modulating the function and specificity of SAK–Pm activator complex by maintaining the precise orientation of $SAKHis^{43}$-$\mu PmTrp^{215}$ pair near the active site of Pm.

Acknowledgements

Authors would like to thank Council of Scientific and Industrial Research and Department of Biotechnology, Govt. of India for the financial support.

Appendix A. Supplementary data

Supplementary data associated with this article can be found, in the online version, at doi:10.1016/j.febslet.2012.01.046.

References

[1] Sako, T., Sawaki, S., Sakurai, T., Ito, S., Yoshizawa, Y. and Kondo, I. (1983) Cloning and expression of the staphylokinase gene of *Staphylococcus aureus* in Escherichia coli. Mol. Gen. Genet. 190, 271–277.

[2] Lack, C.H. (1948) Staphylokinase; an activator of plasma protease. Nature 161, 559.

[3] Collen, D. and Van de Werf, F. (1993) Coronary thrombolysis with recombinant staphylokinase in patients with evolving myocardial infarction. Circulation 87, 1850–1853.

[4] Vanderschueren, S. et al. (1995) A randomized trial of recombinant staphylokinase versus alteplase for coronary artery patency in acute myocardial infarction. The STAR Trial Group.. Circulation 92, 2044–2049.

[5] Renatus, M., Engh, R.A., Stubbs, M.T., Huber, R., Fischer, S., Kohnert, U. and Bode, W. (1997) Lysine 156 promotes the anomalous proenzyme activity of tPA: X-ray crystal structure of single-chain human tPA. EMBO J. 16, 4797–4805.

[6] Collen, D., Schlott, B., Engelborghs, Y., Van Hoef, B., Hartmann, M., Lijnen, H.R. and Behnke, D. (1993) On the mechanism of the activation of human plasminogen by recombinant staphylokinase. J. Biol. Chem. 268, 8284–8289.

[7] Silence, K., Collen, D. and Lijnen, H.R. (1993) Interaction between staphylokinase, plasmin(ogen), and alpha 2-antiplasmin. Recycling of staphylokinase after neutralization of the plasmin–staphylokinase complex by alpha 2-antiplasmin. J. Biol. Chem. 268, 9811–9816.

[8] Reddy, K.N. and Markus, G. (1972) Mechanism of activation of human plasminogen by streptokinase. Presence of active center in streptokinase–plasminogen complex. J. Biol. Chem. 247, 1683–1691.

[9] Grella, D.K. and Castellino, F.J. (1997) Activation of human plasminogen by staphylokinase. Direct evidence that preformed plasmin is necessary for activation to occur. Blood 89, 1585–1589.

[10] Schlott, B., Guhrs, K.H., Hartmann, M., Rocker, A. and Collen, D. (1997) Staphylokinase requires NH_2-terminal proteolysis for plasminogen activation. J. Biol. Chem. 272, 6067–6072.

[11] Rajamohan, G. and Dikshit, K.L. (2000) Role of the N-terminal region of staphylokinase (SAK): evidence for the participation of the N-terminal region of SAK in the enzyme–substrate complex formation. FEBS Lett. 474, 151–158.

[12] Parry, M.A., Zhang, X.C. and Bode, I. (2000) Molecular mechanisms of plasminogen activation: bacterial cofactors provide clues. Trends Biochem. Sci. 25, 53–59.

[13] Rabijns, A., De Bondt, H.L. and De Ranter, C. (1997) Three-dimensional structure of staphylokinase, a plasminogen activator with therapeutic potential. Nat. Struct. Biol. 4, 357–360.

[14] Parry, M.A., Fernandez-Catalan, C., Bergner, A., Huber, R., Hopfner, K.P., Schlott, B., Guhrs, K.H. and Bode, W. (1998) The ternary microplasmin–staphylokinase–microplasmin complex is a proteinase-cofactor–substrate complex in action. Nat. Struct. Biol. 5, 917–923.

[15] Wang, X., Lin, X., Loy, J.A., Tang, J. and Zhang, X.C. (1998) Crystal structure of the catalytic domain of human plasmin complexed with streptokinase. Science 281, 1662–1665.

[16] Jespers, L., Van Herzeele, N., Lijnen, H.R., Van Hoef, B., De Maeyer, M., Collen, D. and Lasters, I. (1998) Arginine 719 in human plasminogen mediates formation of the staphylokinase:plasmin activator complex. Biochemistry 37, 6380–6386.

[17] Dahiya, M., Singh, S., Rajamohan, G., Sethi, D. and Ashish and Dikshit, K.L. (2011) Intermolecular interactions in staphylokinase–plasmin(ogen) bimolecular complex: Function of His43 and Tyr44. FEBS Lett. 585, 1814–1820.

[18] Rajamohan, G., Dahiya, M., Mande, S.C. and Dikshit, K.L. (2002) Function of the 90-loop (Thr90-Glu100) region of staphylokinase in plasminogen activation probed through site-directed mutagenesis and loop deletion. Biochem. J. 365, 379–389.

[19] Deutsch, D.G. and Mertz, E.T. (1970) Plasminogen: purification from human plasma by affinity chromatography. Science 170, 1095–1096.

[20] Jackson, K.W., Esmon, N. and Tang, J. (1981) Streptokinase and staphylokinase. Methods Enzymol. 80 Pt C, 387–394.

[21] Shibata, H., Nagaoka, M., Sakai, M., Sawada, H., Watanabe, T. and Yokokura, T. (1994) Kinetic studies on the plasminogen activation by the staphylokinase–plasmin complex. J. Biochem. 115, 738–742.

[22] Aneja, R., Datt, M., Singh, B., Kumar, S. and Sahni, G. (2009) Identification of a new exosite involved in catalytic turnover by the streptokinase–plasmin activator complex during human plasminogen activation. J. Biol. Chem. 284, 32642–32650.

[23] Sakharov, D.V., Lijnen, H.R. and Rijken, D.C. (1996) Interactions between staphylokinase, plasmin(ogen), and fibrin. Staphylokinase discriminates between free plasminogen and plasminogen bound to partially degraded fibrin. J. Biol. Chem. 271, 27912–27918.

[24] Hutsell, S.Q., Kimple, R.J., Siderovski, D.P., Willard, F.S. and Kimple, A.J. (2010) High-affinity immobilization of proteins using biotin- and GST-based coupling strategies. Methods Mol Biol 627, 75–90.

[25] Papalia, G. and Myszka, D. (2010) Exploring minimal biotinylation conditions for biosensor analysis using capture chips. Anal Biochem 403, 30–35.

[26] Hodsdon, M.E., Ponder, J.W. and Cistola, D.P. (1996) The NMR solution structure of intestinal fatty acid-binding protein complexed with palmitate: application of a novel distance geometry algorithm. J. Mol. Biol. 264, 585–602.

[27] Ren, P. and Ponder, J.W. (2003) Polarizable Atomic Multipole Water Model for Molecular Mechanics Simulation. J. Phys. Chem. B 107, 5933–5947.

[28] Guex, N. and Peitsch, M.C. (1997) SWISS-MODEL and the Swiss-PdbViewer: an environment for comparative protein modeling. Electrophoresis 18, 2714–2723.

[29] Crowley, P.B. and Golovin, A. (2005) Cation–pi interactions in protein–protein interfaces. Proteins 59, 231–239.